

First order particle acceleration in magnetically-driven flows

Andrey Beresnyak and Hui Li

Los Alamos National Laboratory, Los Alamos, NM, 87545

We demonstrate that particles are regularly accelerated while experiencing curvature drift in flows driven by magnetic tension. Some examples of such flows include spontaneous turbulent reconnection and decaying magnetohydrodynamic (MHD) turbulence, where magnetic field relaxes to a lower-energy configuration and transfers part of its energy to kinetic motions. The opposite process, such as dynamo, will actually result in the net cooling of particles by the curvature drift. Being very generic, this acceleration mechanism is likely to be responsible in production of non-thermal particle distribution in magnetically-dominant environments such as solar chromosphere, pulsar magnetosphere, jets from supermassive black holes, γ -ray bursts, etc.

PACS numbers: 52.65.Kj, 52.30.Cv, 47.27.Jv, 95.30.Qd, 52.35.Ra, 47.27.E-, 52.30.Cv

Introduction — In addition to direct acceleration by electric fields, particle acceleration is classified into “first order Fermi” mechanism where particles are gaining energy regularly, e.g., by colliding with converging magnetic mirrors and “second order Fermi” where particles can both gain and lose energy [1]. The second order process represents diffusion in energy space and can be slow. The first order mechanism usually dominates, if present. The outcome of acceleration depends on the rate at which particle gain energy, called acceleration rate r_{acc} and the rate of particle escape from the system, r_{esc} . If escape is negligible and r_{acc} is constant with energy, the energy grows exponentially. Also, if r_{esc}/r_{acc} does not depend on energy, the stationary solution for the particle distribution is a power-law, with the power law index determined by $-1 - r_{esc}/r_{acc}$, see, e.g. [2]. Various environments, such as supernova shocks, were thought to satisfy this condition and produce power-law distributed cosmic rays, consistent with observations [3]. Acceleration within many orders of magnitude in energy was regarded as a result of a large-scale physical layout of the acceleration site, e.g., the planar shock can be thought of as a set of large-scale converging mirrors. The same picture could also be applied to the large-scale reconnection site, where the two sides of the inflow effectively work as converging mirrors [4]. In this Letter we deviate from this mindset and try to find regular acceleration over large energy ranges in systems that do not necessarily possess global regular structure.

Magnetically-dominated environments are fairly common in astrophysics and we know that energy can be dissipated even in nearly inviscid and nearly perfectly conductive astrophysical environments due to the presence of turbulence. At the same time, it was realized that shock acceleration might not be as ubiquitous, especially in tenuous and relativistic astrophysical plasmas, which are less likely to produce shocks. Observations of certain highly variable astrophysical objects suggested extremely fast acceleration timescales, thought to be incompatible with diffusive shock acceleration [5, 6]. In this situation it would be especially interesting to find how magnetic

energy can be transferred into particle energy. Recently, both MHD fluid simulations [7] and ab-initio plasma simulations [8, 9] of reconnection demonstrated regular acceleration and it is important to understand the physical mechanism behind this effect.

Normally, turbulent environments are expected to be regions of fairly slow second-order acceleration, see, e.g., [10]. Here we argue that the transfer of energy from magnetic field to kinetic motions and the curvature drift acceleration are inherently related, so that in systems with the average positive energy transfer from magnetic energy to kinetic motions there is an average positive curvature drift acceleration, while in the opposite case, there is an average curvature drift cooling.

One of the commonly considered cases of magnetically-driven flows is magnetic reconnection. A significant effort was put into understanding on non-ideal plasma effects that could both cause reconnection and create non-zero parallel component of the electric field [11, 12]. While non-ideal effects are indeed required for the individual field lines to break and reconnect, their influence is limited to fairly small scales, typically below the ion skin depth d_i . In this Letter, we instead focus on larger scales and ignore non-ideal effects for the following two reasons. Firstly, it has been argued that understanding of global energetics of large-scale reconnection does not necessarily require detailed knowledge on how individual field lines break and reconnect [13–16]. Secondly, in order to understand high energy particle acceleration, one normally has to consider plasma dynamics on scales much larger than d_i , that is on MHD scales.

MHD flows and energy transfer — Well-conductive plasmas can be described on large scales as inviscid and perfectly conducting fluid (ideal MHD). The ideal MHD equations allows for exchange between thermal, kinetic and magnetic energies. The Lorentz force density, multiplied by the fluid velocity, $\mathbf{u} \cdot [\mathbf{j} \times \mathbf{B}]/c$ is the amount of energy transferred from magnetic to kinetic energy. While total energy is supposed to be conserved in the ideal MHD, it is not the case in real systems that might have vanishing, but non-zero dissipation co-

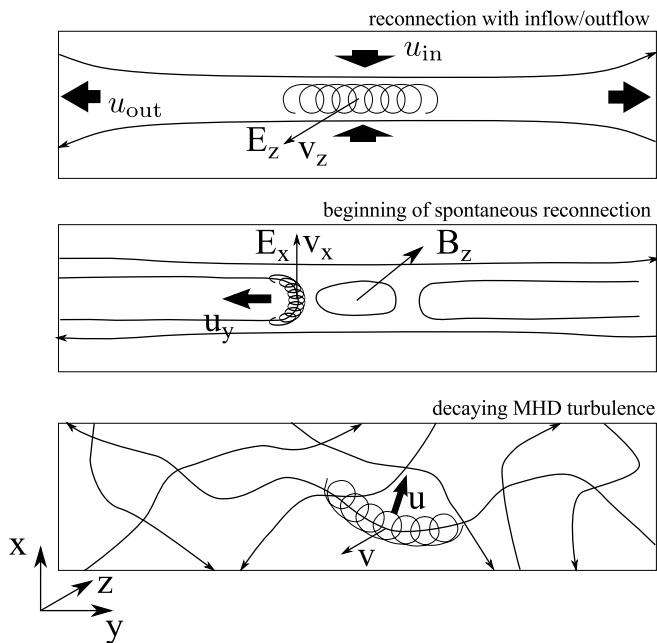


FIG. 1. A cartoon of several acceleration mechanisms in magnetized environments. The upper panel depicts reconnection with inflow and outflow where particles can be accelerated regularly due to the gradient drift and the large-scale electric field. The acceleration term is dominated by v_z and E_z . The middle panel depicts initial stages of spontaneous reconnection which has negligible inflow where the above gradient drift term averages out. In this case acceleration is mostly driven by contracting field lines which drive fluid motion and at the same time cause the curvature drift of particles. Note that the direction of drift is typically perpendicular to the fluid motion. The dominant acceleration term is associated with E_x and the field curvature of B_y component. The bottom panel depicts the same mechanism in a more homogeneous and isotropic setup of decaying MHD turbulence, which also has contracting field lines. In this situation all vector components contribute equally.

efficiently. This is qualitatively explained by the nonlinear turbulent cascade that brings energy to smaller and smaller scales until it dissipates. One of the important examples of this is the spontaneous reconnection where the thin current layer becomes turbulent and starts dissipating magnetic energy at a constant rate. The small scales of these turbulent flows resemble “normal” MHD turbulence which has equipartition between magnetic and kinetic energies [16]. In order to feed the turbulent cascade with magnetic energy, approximately half of it has to be transferred into kinetic motions. This requires that in turbulence fed by magnetic energy the term $\mathbf{u} \cdot [\mathbf{j} \times \mathbf{B}]/c$ must be *positive on average* and could be approximated as half of the volumetric energy dissipation rate. This term can be rewritten as $-(\mathbf{u} \cdot \nabla)B^2/8\pi + \mathbf{u} \cdot (\mathbf{B} \cdot \nabla)\mathbf{B}/4\pi$, where the first term is the advection of magnetic energy by the fluid, while the second term is the actual energy transfer. For the

purpose of future calculations we will separate the last term in the following way:

$$\mathcal{T} = \frac{1}{4\pi} \mathbf{u} \cdot (\mathbf{B} \cdot \nabla)\mathbf{B} = \frac{1}{4\pi} (\mathbf{u} \cdot \mathbf{B})(\mathbf{b} \cdot \nabla)B + \frac{B}{4\pi} \mathbf{u} \cdot (\mathbf{B} \cdot \nabla)\mathbf{b} = \mathcal{X} + \mathcal{D}, \quad (1)$$

where we designated $\mathbf{b} = \mathbf{B}/B$, a unit magnetic vector. We designate the term \mathcal{X} containing cross helicity density $\mathbf{u} \cdot \mathbf{B}$ as a cross-helical term and argue that it is not sign-definite and often averages out in mirror-symmetric systems. The second term \mathcal{D} contains magnetic field curvature $(\mathbf{B} \cdot \nabla)\mathbf{b}$ and will be important for subsequent calculation of curvature drift.

Curvature drift — Particles motion in slowly-varying electric and magnetic field can be described in the so-called drift approximation. The leading drift terms are known as electric, gradient and curvature drifts. While electric drift, proportional to $[\mathbf{E} \times \mathbf{B}]$, can not produce acceleration, the other two drifts can. For example, imagine the configuration of the reconnection with the inflow, Fig 1 top panel. The gradient drift $\sim [\mathbf{B} \times \nabla|B|]$ is along $-z$, and so is the electric field in the ideal case $E = -[\mathbf{u} \times \mathbf{B}]/c$. Their product will be positive and will result in acceleration which is due to particles being compressed by the converging inflow. This mechanism does not work in the initial, most energetic stages of spontaneous reconnection which has negligible inflow, Fig. 1 middle panel [16]. It is this initial stage that has the highest volumetric dissipation rate, however. Fig 1 illustrates why curvature drift acceleration is important in this configuration. It also turns out that in any magnetically-driven turbulent environment, such as depicted on the bottom panel of Fig 1, curvature drift acceleration will accelerate particles on average.

Let us look carefully at the term which is responsible for acceleration by curvature drift, $d\mathcal{E}/dt = -2(\mathcal{E}_{\parallel}/B)[\mathbf{u} \times \mathbf{B}] \cdot [\mathbf{b} \times (\mathbf{b} \cdot \nabla)\mathbf{b}]$, see, e.g., [17], where $\mathcal{E}_{\parallel} = v_{\parallel}p_{\parallel}/2 = \gamma mv_{\parallel}^2/2$ is a particle’s parallel kinetic energy. With some manipulation, this expression could be equivalently transformed as $2(\mathcal{E}_{\parallel}/B)\mathbf{u} \cdot (\mathbf{B} \cdot \nabla)\mathbf{b}$. It now becomes clear that this term is related to the transfer rate between magnetic and kinetic energies, in particular it is a fraction of \mathcal{D} :

$$\frac{d\mathcal{E}}{dt} = \mathcal{E}_{\parallel} \frac{8\pi}{B^2} \mathcal{D}. \quad (2)$$

The physical meaning of this equation is that, given efficient particle scattering, so that $\mathcal{E}_{\parallel} = \mathcal{E}/2$, the acceleration rate is determined by the half of the local energy transfer rate $8\pi\mathcal{D}/B^2$, not including the \mathcal{X} term.

A case study — We can test the general ideas outlined above in two physical cases that feature turbulent energy transfer from magnetic to kinetic energies. Using

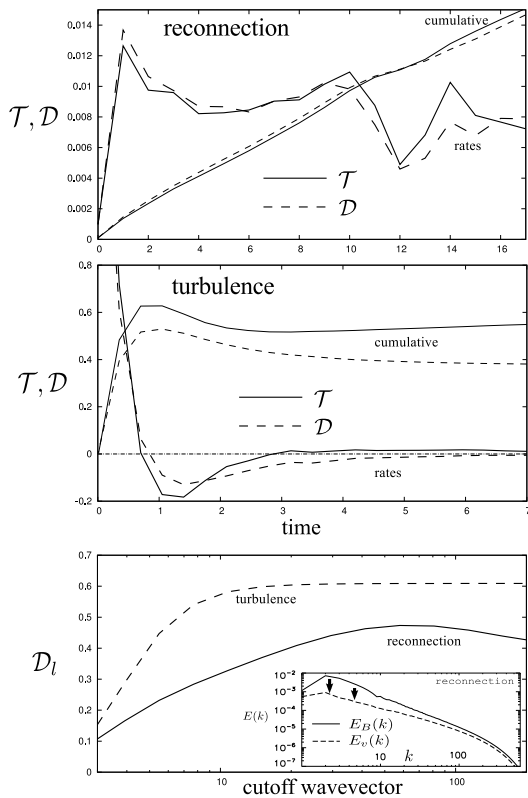


FIG. 2. A case study of curvature drift acceleration and energy conversion in spontaneous reconnection and decaying MHD turbulence. Top and middle panel: total energy conversion rate \mathcal{T} and curvature acceleration rate \mathcal{D} in arbitrary units. Cumulatives $\int \{\mathcal{T}, \mathcal{D}\} dt$ are also shown. While reconnection case (upper panel) shows relatively stable rates, the decaying turbulence (middle panel) feature burst of energy conversion within a few Alfvénic times. In both cases the gradient drift acceleration does not contribute significantly. Bottom panel shows the scale-dependency of the \mathcal{D}_l term. This term is approximately constant for all small scales until l reaches scales at which magnetic energy is converted into kinetic. The inset in the bottom panel shows kinetic and magnetic energy spectra in spontaneous reconnection [16] with thick arrows showing the energy transfer.

spontaneous reconnection and the decaying MHD turbulence simulated numerically, we can directly calculate the discussed terms and compare them. The spontaneous reconnection numerical experiment was started with thin planar current sheet and small perturbations in \mathbf{u} and \mathbf{B} and was described in detail in [16], while the decaying MHD turbulence was similar to our previous incompressible driven simulations in [18], except that there was no driving and the initial conditions were set as a random magnetic field with wavenumbers $1 < k < 5$ and zero velocity. Both simulations developed magnetically-driven flows, from which we calculated the average \mathcal{T} , \mathcal{D} , and \mathcal{X} terms and presented them in Fig. 2.

The spontaneous reconnection case had fairly stable reconnection rate, this also corresponded to the approx-

imately constant \mathcal{D} integrated over the volume. The \mathcal{X} term didn't seem to be sign-definite and contributed relatively little. Gradient drift acceleration was also negligible, possibly due to the absence of global compression. Keeping in mind that all the energy had to come from magnetic energy, and given that the dissipation rate was approximately constant, it was no surprise that the average \mathcal{D} term evolved relatively little. It should be noted, however, that in the spontaneous reconnection experiment the width of the reconnection region was growing approximately linear with time [16], so the \mathcal{D} term magnitude, pertaining to the reconnection region itself was much higher than that of an averaged \mathcal{D} over the total volume. Given the reconnection layer thickness $l(t)$, the local \mathcal{D} could be estimated as $(1/2)\rho v_r v_A^2 / l(t)$, where v_r is a reconnection rate, which was $v_r \approx 0.015 v_A$ in [16] and the $1/2$ comes from only half of magnetic energy being transferred into kinetic energy before physically dissipating on very small dissipation scale $\eta \ll l(t)$. This would correspond to acceleration rate of $(1/4)v_r/l(t)$ and can be very high, because the $l(t)$ could be as small as the Sweet-Parker current sheet width or the ion skin depth.

The decaying MHD turbulence experienced two regimes: 1) the initial oscillation when excessive amount of magnetic energy was converted into kinetic energy and the bounce back and partial inverse conversion afterwards; 2) the self-similar decay stage of MHD turbulence. The first stage had the strongest conversion term which was dominated by \mathcal{D} . All terms integrated over time were mostly accumulated within the first 1-2 Alfvénic times.

Scale-filtered quantities — It is known from turbulence theory that the energy transfer rate \mathcal{T} can be demonstrated to be local in scale, under relatively weak assumptions [19]. The scale-locality means that each scale contributes to the transfer independently. We also know empirically that most of the transfer between magnetic and kinetic energies happens on relatively large scales which are comparable to the outer scale of the system, while below outer scale there is little average transfer due to an approximate equipartition between kinetic and magnetic energies. For example, the reconnecting turbulent current layer has most of its \mathcal{T} transfer within a factor of a few of the scale of the layer thickness, while in the decaying turbulence problem it is within a factor of a few from the outer scale of the system. Let us designate \mathcal{T}_l as a transfer calculated from quantities which were filtered by low-pass Gaussian filter with a cutoff wavenumber of $1/l$. Keeping in mind of locality we will conclude that only scales larger than l will contribute to \mathcal{T}_l . This means that \mathcal{T}_l will be constant for small l and will start decreasing when l approaches the outer scale of the problem L . In general, we can not deduce the same for \mathcal{D}_l and \mathcal{X}_l , but keeping in mind that \mathcal{X}_l contributes relatively little in two cases that we considered, $\mathcal{D}_l \approx \mathcal{T}_l$ in those cases. Fig. 2 demonstrates this behavior on the bottom panel, where energy transfer is operating between

wavenumbers 2 and 20 in the reconnection case ($1/20$ is approximately the layer width at this point), and the \mathcal{D}_l mostly changes within the same range of scales. The decaying turbulence case has the transfer more localized around the outer scales.

In terms of drift, the particle with Larmor radius r_L will “feel” magnetic and electric fields on scales larger than r_L , while the scales smaller or equal to r_L will contribute to particle scattering. We will presume, therefore, that \mathcal{D}_{r_L} is constant below a certain energy and so is the acceleration rate, due to the arguments above. A similar, more hand-waving argument, is that the term \mathcal{D}_l could be roughly approximated as $B_l^2 v_l / l$, resembles turbulent energy transfer rate, which is scale-independent. Interestingly, starting with scale independent energy transfer in turbulence we arrived at the energy-independent acceleration rates. Given the generality of the arguments presented above it is not surprising that energy-independent rates were indeed observed in simulations [9].

Acceleration in spontaneous reconnection — The development of the thin current sheet instability results in turbulence and reconnection in a sense of dissipated magnetic energy. This process will come through two distinct regimes, the regime without significant outflow for times smaller than L/v_A [16] and the stationary reconnection with outflow for larger times [13]. Let us consider the first regime which has larger dissipation rate per unit volume, because the current layer thickness $l(t) = v_r t$ is relatively small. We use v_r for the reconnection rate and t as the time since the beginning of spontaneous reconnection. Let us assume that the current layer thickness is limited from below by the ion skin depth. We will have acceleration rate of $1/(4t)$ for all times larger than d_i/v_r but smaller than L/v_A . The solution for energy, therefore, will be $\mathcal{E} = \mathcal{E}_0 (tv_r/d_i)^{1/4}$ where \mathcal{E}_0 is the initial energy, e.g., the thermal energy. The particle’s energy will be $\mathcal{E}_{max} = 0.35\mathcal{E}_0(L/d_i)^{1/4}$ given the reconnection rate $v_r = 0.015v_A$. This, however, is only the maximum energy of accelerated particles, as only a tiny fraction of particles were contained in the original thin current sheet and started accelerated from initial time d_i/v_r [9]. With proper stochastic treatment and assuming that the escape rate r_{esc} is negligible compared with acceleration rate in this no-outflow problem, we expect to see the power law particle spectrum with the -1 slope and a cutoff at \mathcal{E}_{max} .

The subsequent development of an outflow will do three things: first it will enable the inflow and therefore the extra acceleration term associated with gradient drift or converging magnetic mirrors [4]. Secondly, it will stabilize acceleration rate for the curvature drift acceleration at $v_A/4L$, as the current layer is no longer expanding. Thirdly, it will enable particle escape through the outflow. In this regime the spectrum will extend from \mathcal{E}_{max} to higher energies, up to Larmor radii of the large scale of the current sheet L . The spectral slope

of this extension will be determined by $-1 - r_{esc}/r_{acc}$, where r_{acc} should account for all acceleration and cooling mechanisms, such as gradient drift acceleration and outflow cooling. The detailed analysis of this stage will be the subject of a future work.

The electron spectra observed in solar X-ray flares are fitted with the thermal component with temperature of several keV and the steep power law component. This is consistent with our picture, as the rather shallow -1 slope, containing most of its energy near \mathcal{E}_{max} , is likely to thermalize. Also, the outflow phase will extend this distribution as a power-law to higher energies.

Discussion — We demonstrated that magnetic configurations that relax to the lower states of magnetic energy will also regularly accelerate particles, on timescales which are, typically, Alfvénic, but can be much shorter, e.g., in the beginning of spontaneous reconnection. As formation of thin current sheets due to nonlinearity is relatively common [20], we expect efficient injection of particles which are supra-thermal by a factor of $(L/d_i)^{1/4}$ from such places. Injected particles will be further accelerated by large-scale magnetically driven flows. This is potentially interesting with connection to acceleration in a number of high energy astrophysical systems. Recent observations of gamma-ray flares from Crab [5] have suggested that reconnection could be needed to explain the impulsive nature of the energy release and the associated particle acceleration [21]. Some radio jets powered by supermassive black holes exhibit ~ 10 min variations in TeV emissions, e.g., [6]. Such fast time variabilities, along with other emission region constraints, have been argued in [22] as being evidence for mini-jets generated by reconnection. Particle acceleration during reconnection is a topic under intense study, but the mechanism discussed in this Letter is distinctly different from the direct acceleration by the reconnecting electric field at the X-line. In fact, we completely ignore non-ideal effects which produce local $\mathbf{E} \parallel \mathbf{B}$. Also, our mechanism is not tied to a special X-point, but instead volumetric.

The regular acceleration due to converging field lines have been suggested in [4], later it was pointed by [23] that an outflow cooling should also be included. The acceleration in turbulent reconnection has been further numerically studied in [7]. Plasma PIC simulations has also been increasingly used to understand particle acceleration. The emphasis was mostly on the non-ideal effects near X-line regions and interaction with magnetic islands [11, 12, 24–26]. The change of energy due to curvature drift in a single collision of a particle with magnetic island was estimated analytically in [25]. An important question that was left out was whether it will be acceleration or cooling on average. Without understanding this it was not clear whether the acceleration is efficient first-order regular acceleration or not. This Letter unambiguously answers this question by tying it to the direction of energy transfer from magnetic to kinetic. We also showed

that the curvature drift acceleration does not require particles to be trapped in contracting magnetic islands, so their energy is not limited by this requirement.

PIC simulations are limited in the range of scales and energies they cover. Recent simulations in [8, 9] demonstrated acceleration up to 100 MeV in electron energies, which is below maximum energy in most astrophysical sources. Theory, therefore, is necessary to supplement conjectures based on the observed PIC distribution tails, explaining the underlying physical mechanism and making predictions for astrophysical systems which often feature gigantic scale separation between plasma scales and the size of the system. The feedback from simulations, nevertheless, was very useful, in particular the recent simulations [9] that reached MHD scales and confirmed the prediction that the curvature drift acceleration will dominate compared to the non-ideal electric field acceleration.

Acknowledgements — We are grateful to Fan Guo for sharing his results on a preliminary stage. The work is supported by the LANL/LDRD program and the DoE/Office of Fusion Energy Sciences through CMSO. Computing resources at LANL are provided through the Institutional Computing Program. We also acknowledge support from XSEDE computational grant TG-AST110057.

-
- [1] E. Fermi, *Physical Review* **75**, 1169 (1949).
 - [2] L. O. Drury, P. Duffy, D. Eichler, and A. Mastichiadis, *A&A* **347**, 370 (1999).
 - [3] G. F. Krymskii, *Soviet Physics Doklady* **22**, 327 (1977).
A. R. Bell, *MNRAS* **182**, 147 (1978).
M. A. Malkov and L. O’C Drury, *Reports on Progress in Physics* **64**, 429 (2001).
 - [4] E. M. de Gouveia dal Pino and A. Lazarian, *A&A* **441**, 845 (2005).
 - [5] A. Abdo *et al.*, *Science* **331**, 739 (2011).
 - [6] F. Aharonian *et al.*, *A&A* **464**, 235 (2007).
J. Aleksić *et al.*, *ApJ* **730**, L8 (2011).
 - [7] G. Kowal, E. M. de Gouveia Dal Pino, and A. Lazarian, *Physical Review Letters* **108**, 241102 (2012).
 - [8] L. Sironi and A. Spitkovsky, *ApJ* **783**, L21 (2014).
 - [9] F. Guo, H. Li, W. Daughton, and Y.-H. Liu, arXiv:1405.4040 (2014).
 - [10] R. Schlickeiser, *Cosmic Ray Astrophysics* (Springer, Berlin, 2002).
J. Cho and A. Lazarian, *Astrophys. J.* **638**, 811 (2006).
 - [11] P. Pritchett, *Journal of Geophysical Research: Space Physics* (1978–2012) **111**, 10212 (2006).
 - [12] X. Fu, Q. Lu, and S. Wang, *Physics of Plasmas* (1994–present) **13**, 012309 (2006).
 - [13] A. Lazarian and E. T. Vishniac, *Astrophys. J.* **517**, 700 (1999).
 - [14] G. L. Eyink, A. Lazarian, and E. T. Vishniac, *Astrophys. J.* **743**, 51 (2011).
 - [15] N. F. Loureiro, A. A. Schekochihin, and S. C. Cowley, *Physics of Plasmas* **14**, 100703 (2007).
 - [16] A. Beresnyak, arXiv:1301.7424 (2013).
 - [17] D. V. Sivukhin, *Reviews of Plasma Physics* **1**, 1 (1965).
 - [18] A. Beresnyak and A. Lazarian, *Astrophys. J.* **702**, 1190 (2009).
 - [19] H. Aluie and G. L. Eyink, *Phys. Rev. Lett.* **104**, 081101 (2010).
A. Beresnyak, *Phys. Rev. Lett.* **108**, 035002 (2012).
 - [20] E. Parker, *Spontaneous current sheets in magnetic fields: with applications to stellar x-rays* (Oxford University Press, USA, 1994).
 - [21] E. Clausen-Brown and M. Lyutikov, *Monthly Notices of the Royal Astronomical Society* **426**, 1374 (2012).
 - [22] D. Giannios, *MNRAS* **431**, 355 (2013).
 - [23] L. O. Drury, *MNRAS* **422**, 2474 (2012).
 - [24] S. Zenitani and M. Hoshino, *The Astrophysical Journal Letters* **562**, L63 (2001).
 - [25] J. F. Drake, M. Swisdak, H. Che, and M. A. Shay, *Nature (London)* **443**, 553 (2006).
 - [26] M. Oka *et al.*, *The Astrophysical Journal* **714**, 915 (2010).